The Modulation of the Period of the Quasi-Biennial Oscillation by the Solar Cycle

Le Kuai[1*], Run-Lie Shia[1], Xun Jiang[2], Ka-Kit Tung[3], Yuk L. Yung[1]

1 Division of Geological and Planetary Sciences, California Institute of Technology, Pasadena, CA 91125

2 Department of Earth and Atmospheric Sciences, University of Houston, TX 77204

3 Department of Applied Mathematics, University of Washington, Seattle, WA 98195

* To whom all correspondence should be addressed. E-mail:kl@gps.caltech.edu

Submitted to *J. Atmos. Sci*

Abstract

Using a two-and-a-half dimensional THINAIR model, we examine the mechanism of solar-cycle modulation of the Quasi-Biennial Oscillation (QBO) period. Previous model results (using 2D and 3D models of varying complexity) have not convincingly established the proposed link of longer QBO periods during solar minima. Observational evidence for such a modulation is also controversial because it is only found during a period (1960s to early 1990s), which is contaminated by volcanic aerosols. In the model, 400-year runs without volcano influence can be obtained, long enough to establish some statistical robustness. Both in model and observed data, there is a strong synchronization of the QBO period with integer multiples of the Semi-Annual Oscillation (SAO) in the upper stratosphere. Under the current level of wave forcing, the period of the QBO jumps from one multiple of SAO to another and back so that it averages to 28 months, never settling down to a constant period. The "decadal" variability in the QBO period takes the form of quantum jumps and these however do not appear to follow the level of the solar flux in either the observation or the model using realistic quasi-periodic solar cycle (SC) forcing. To understand the solar modulation of the QBO period, we perform model runs with a range of perpetual solar forcing, either lower or higher than the current level. At the current level of solar forcing, the model QBO period consists of a distribution of 4-SAO periods and 5-SAO periods, similar to the observed distribution. This distribution changes as solar forcing changes. For lower (higher) solar forcing, the distribution shifts to more (less) 4-SAO periods than 5-SAO periods. The record-averaged QBO period increases with the solar forcing. However, because this effect is rather weak and is detectable only with exaggerated forcing, we suggest that the previous result of the anti-correlation of the QBO period with the SC seen in short observational records reflects only a chanced behavior of the QBO period,

which naturally jumps in a non-stationary manner even if the solar forcing is held constant, and the correlation can change as the record gets longer.

1. Introduction

Quasi-Biennial Oscillation (QBO) is an internal oscillation of the equatorial zonal wind in the stratosphere involving wave-mean flow interactions (Holton and Lindzen, 1972; Dunkerton, 1997; Baldwin *et al.*, 2001). There have been numerous observational studies of the QBO in the zonal wind, temperature, and ozone (e.g., Angell and Korshover, 1970; Oltmans and London, 1982; Hasebe, 1983; Zawodny and McCormick, 1991; Randel et al., 1996; Pawson and Fiorino, 1998). The period of the QBO averages to about 28 months but is known to have inter-annual variations of a few months about the average. While it is not surprising for this phenomenon arising from wave-mean flow interaction to have a variable period, the possibility that it could be affected by external forcing such as the 11-year solar cycle (SC) is intriguing.

Using radiosonde data from Free University of Berlin (FUB) near the equator at 45 hPa between 1956-1996, Salby and Callaghan (2000) found that the duration of the equatorial westerly phase QBO (w-QBO) appears to vary with the SC and tends to be longer during the solar minima (SC-min; we will use "SC-max" to refer to solar maxima). By comparison, the duration of the easterly phase of QBO (e-QBO) has little variability at that level, but has a decadal variation above 30 hPa. Soukharev and Hood (2001) extended the work of Salby and Callaghan (2000) using composite mean analysis of a similar dataset but at 50 to 10 hPa from 1957 to 1999. Their analysis also indicated that the duration of both QBO phases is longer during the SC-min. Pascoe *et al.*, (2005) examined the ERA-40 data set (Uppala *et al.*, 2005) from 1958 to 2001 to study the solar modulation of the mean descent rate of the shear zone. They found that on average, it requires two more months for the easterly shear zone to descend from 20 to 44 hPa under the SC-min condition and that the w-QBO duration increases (decreases) under the SC-min (SC-max) condition. This relation, however, broke down during the 1990s. Later, Hamilton (2002) and Fischer and Tung (2008) employed longer FUB datasets and both found the opposite behavior in the 1950s, the late 1990s and 2000s. Although there is anti-correlation (correlation coefficient = -0.46) between the w-QBO duration at 50 hPa and the solar flux for the period of 1956-1996, Hamilton (2002) showed that the correlation coefficient is only -0.1 during the extended period of 1950-2001. Additionally, Fischer and Tung (2008), who applied the Continuous Wavelet Transform to determine the QBO period at 50 hPa for the longer record of 1953-2007, found that the correlation coefficient between the period of the QBO and a SC is practically zero. These later work did not contradict the findings of the earlier authors. They merely pointed out that the behavior of the 60s, 70s, 80s and early 90s were the opposite to that of the other decades before and after this period. A possible cause may be that the diabatic heating due to volcanic aerosols could lead to the stalling of the downward propagation of the QBO (Dunkerton, 1983). Fischer and Tung (2008) found that in the recent two decades when no large volcanic eruptions occurred, the previous anti-correlation disappeared and reverted to a positive correlation, which was also found prior to the 1960s. A few more decades without volcanic interference would be needed to obtain a statistically significant correlation with the SC. This complication can be circumvented in a modeling experiment.

An additional possibility considered here is that, with or without volcano aerosols in the stratosphere, the QBO period may respond to the solar-flux in a non-stationary manner, with apparently random changes even without being perturbed by external forcing. The averaged effect on the QBO period by the solar-cycle forcing is detectable only if the record is over a hundred years long. Although such a long record is not available in observation, model results of over 200 years can be generated to test this hypothesis.

2. Relevant Features in ERA-40 Data

There are two characteristics of the observed behavior of the QBO that are relevant to the present study but have been underemphasized by previous modeling and observational discussions: its synchronization with the Semi-Annual Oscillation (SAO) in the upper stratosphere and the apparently random quantum jumps of the QBO period by one multiple of the SAO period. A detailed description of these features in the ERA-40 data and an explanation of possible causes can be found in Kuai *et al.,* (2008). Here we briefly summarize the observational results for the purpose of comparing with our model results. Fig. 1 shows the equatorial zonal wind as a function of height (up to 1 hPa) and years using ERA-40 data. The upper two panels display the original monthly mean data. For the lower two panels, in the region 1-3 hPa, where SAO and QBO coexist, the QBO is removed by long-term averaging. Only a climatological seasonal cycle, which shows the SAO prominently without the QBO, is displayed in the 1-3 hPa region. Below that the "raw" ERA-40 monthly zonal wind is again shown. A prominent SAO exists near the stratopause level and appears to be synchronized with the QBO below 5 hPa. That is, the w-QBO is initiated from a westerly phase of the SAO (w-SAO), and the next QBO period starts when another w-SAO, four or five SAO periods later, descends below 10 hPa. Therefore, the QBO period is always an integer multiple of the SAO period, since the former always starts with the westerly descent of a SAO. In Fig. 2, we count the number QBO period at 5 hPa in units of SAO periods, ignoring the cases when the SAO fails to initiate a QBO below 10 hPa, and it becomes immediately apparent that the QBO period varies in a non-stationary manner, taking quantum jumps from 4-SAO periods to 5-SAO periods. Such variations are not correlated or anti-correlated with the SC (see the index of Total Solar Irradiance (TSI) plotted at the bottom of Fig. 2(a). Fig. 2(c) shows that there is very little vertical variation (within ~ ±1 month between 1-40 hPa) of the QBO period in the ERA-40 data (see also Fischer and Tung (2008)).

3. The Model

The THINAIR (Two and a Half dimensional INterActive Isentropic Research) is an isentropic chemical-radiative-dynamical model. The model has zonally averaged radiation, chemistry and dynamics and includes the three longest planetary waves, which are prescribed by observations at the tropopause level (Kinnersley and Harwood, 1993). For this study, the planetary wave forcing at the tropopause is fixed at the 1979 year level derived from NCEP reanalysis data (Kalnay, *et al.*, 1996; Kistler, *et al.*, 2001), annually periodic and repeated for all years. This choice reduces inter-annual variability of the planetary wave forcing, so that the (weak) influence of the SC on the QBO can be studied. It removes tropospheric variability of planetary waves, but retains stratospheric variability that is internally generated through wave-mean flow interaction and modulated by SC. The model uses an isentropic vertical coordinate above 350 K. Below 350 K a hybrid coordinate is used to avoid intersection of the coordinate layers with the ground. The version used in this study has 29 layers from the ground to ~100 km for dynamics and 17 layers from ground to ~60 km for chemistry. The model has 19 meridional grid points evenly distributed from pole to pole. The QBO source term in the momentum equation uses parameterization of wave momentum fluxes from Kelvin, Rossby-gravity and gravity waves (Kinnersley and Pawson, 1996). These momentum sources also force the SAO above the QBO. UARS/SUSIM spectral irradiance observation is used for the 11-year SC. UARS/SUSIM data consists of the solar spectrum in 119-400 nm during 1991-2002, with 1-nm resolution. The monthly data are extended to 1947-2005 using F10.7-cm as a proxy (Jackman, *et al.*, 1996). The yearly averaged data are integrated to give photon fluxes in wavelength intervals appropriate for the THINAIR model. The performance of the model has been reported in the literature (Kinnersley and Pawson, 1996). To avoid redoing the climatology of the model with the new UARS/SUSIM solar spectral forcing, we retain the mean SC forcing (SC-mean) in the original model and multiply it by the ratios (SC-max/SC-mean and SC-min/SC-mean using the UARS/SUSIM data) to create the SC-max forcing and SC-min forcing. This procedure is also necessitated by the fact that while the relative variation over a SC is well measured by the UARS/SUSIM instrument, the mean is not calibrated accurately because of possible long-term instrumental drifts.

4. Model Solar Influence on QBO Period

4.1 Time-varying SC run

400-year runs are made using the realistic, time varying SC forcing for 1964-1995 from UARS/SUSIM (extended as described above) and repeated thereafter. The SC-mean of this record is scaled to the SC-mean of the THINAIR model as described above. Even in this long run, the period of the QBO does not settle down to a fixed number, but still executes apparently random jumps. The behavior of the QBO period is quite similar to the observed discussed above. In particular, the QBO period jumps from 4-SAO periods to 5-SAO periods and back, in a non-stationary manner. Fig. 3 shows a height-time cross section of the zonal-mean zonal wind at the equator from the model for 1×SC-vary case. Fig. 4 shows the distribution of model results for 1×SC-vary case from year 126 to year 172. The number of 5-SAO periods and 4-SAO periods are about equal in this 400-year run. However, in different smaller time segments of about 40-46 years (20 QBOs) corresponding to the period of ERA-40 data, the distribution can shift. In some segments, there are more 5-SAO periods than 4-SAO periods (Fig. 5(c)), as in the EAR-40 data. In other segments of about 40-46 years, it can have equal number of 4-SAO and 5-SAO (Fig. 5(b) or more 4-SAO than 5-SAO (Fig. 5(d)). Therefore we are not too concerned that the 400-year model result has proportionally less 5-SAOs than in the ERA-40 data. Forty five years of the observation are probably too short to establish a robust statistics on the distribution; two hundred years are needed. Some of the results presented below are from the 200-year run.

The correlation of the QBO period with the TSI index is small in the model 200-year run. The correlation coefficient is 0.172, consistent with that in the ERA-40 data of 0.05; neither is statistically significant. This result applies to the entire stratosphere, since the QBO period is almost constant with height in both model and ERA-40 data, within an accuracy of 1 to 2 months (Fischer and Tung, 2008).

4.2 Perpetual solar forcing runs

Additionally, we perform 200-year constant solar-cycle forcing experiments in our model to answer the question of whether the non-stationary nature of the QBO period is caused by the fact that the solar- cycle forcing is time-varying. It should be pointed out that we still have the seasonal cycle in the perpetual solar runs. Fig. 6(c) is similar to Fig. 3 except for the perpetual solar-cycle mean forcing, in the 200-year runs. There are no qualitative differences between the perpetual solar forcing run and the variable solar-cycle forcing run. In particular, the QBO period still jumps irregularly from 4-SAO periods to 5-SAO periods and back. We therefore conclude that the non-stationary nature of the QBO period is not caused by the fact that the solar-cycle forcing is time-varying.

4.3 Exaggerated, perpetual solar-cycle forcing

Fig. 6(a) is for the perpetual 15×SC-min condition. At this low solar forcing, the QBO period is mostly at 4-SAO periods. At the slightly higher, but still low, 10×SC-min forcing, the QBO period consists mostly of 4-SAO periods, with occasionally a 5-SAO period (see Fig. 5(b)). Fig. 5(d) shows the result for the high solar forcing, at 10×SC-max, case. There are now more 5-SAO periods than 4-SAO periods. Fig. 6(e) shows the case for still higher SC forcing, at 15×SC-max. The distribution shifts towards even more 5-SAO periods. The histograms for the QBO periods for these five cases are shown in Fig. 7, along with an additional case of 5×SC-max.

In summary, we find that even with perpetual solar forcing, the non-stationary jumps in QBO period continue, with a tendency to jump to longer periods with higher solar forcing. Thus there appears to be some modulation of the QBO period by the SC, but such modulation is only apparent at exaggerated solar forcing. Furthermore, the correlation of solar forcing magnitude and the average QBO period is positive, in contrast to the implication by some previous authors that the QBO period is longer during solar min. In the realistic case of periodic solar-cycle forcing, the instantaneous correlation of the QBO period with the SC is not statistically significant, consistent with the ERA-40 result.

5. Partition of the QBO Period into Westerly and Easterly Durations

In Fig. 8 we plot the QBO period as a function of the solar index in units of solar flux (one unit represents one half of the difference of solar fluxes between the SC-max and SC-min) over the pressure range from 10 to 80 hPa in the model. This establishes that the mean period of the QBO, including its easterly and westerly durations, generally increases as the solar flux increases, contrary to the finding of previous authors that the period reaches a maximum during solar minima. In this model there is no variation of the mean QBO period with height (Panel (a) has lines for 7 levels from 7-80 hPa overlapping and indistinguishable from each other). Above 30 hPa, it is the easterly duration which varies with solar flux (Fig. 8(b), (c) and (d)), while below 50 hPa it is the westerly duration that varies more with solar flux (Fig. 8(e)), consistent with the observational result of Fischer and Tung (2008). The occasional stalling of the easterlies at 30 hPa and the prolongation of the westerly duration at 50 hPa are not seen clearly in these figures because only the average is shown, but these cases can be seen in the height-time diagrams shown previously in Figure 6.

In this model, stalling of the easterly descent tends to occur in some years at around 40 hPa. Below that level, the westerly duration becomes longer in these years. The westerly duration lasts between one to two years. As the solar-cycle flux increases, the westerly duration becomes longer. Therefore it is the average westerly duration near 50 hPa that is correlated with the solar flux, while the easterly duration there shows much smaller variability from one QBO period to the next. Since the next westerly phase is not initiated at the upper stratosphere until the westerly region in the lower stratosphere wanes —due to the filtering of the westerly waves by the lower stratospheric westerly region---the easterly phase above 30 hPa is correspondingly lengthened, and its mean value is correlated with the solar flux. This is consistent with the finding of Salby and Callaghan (2000), except that here the correlation with the solar flux is positive instead of the anti-correlation found by them.

6. Mechanisms for Solar Modulation of QBO Period

As mentioned above, one unique feature of the QBO variability is the apparently random quantum jumps in its period from one SAO multiple to another. This is found in observation and in this model with and without a variable SC forcing. An explanation for this behavior is given in Kuai *et al.* (2008), as a result of the QBO trying to satisfy two often incompatible factors in determining its period: its period as determined internally by the wave forcing amplitude and the wave speed (see Plumb (1977)), and the requirement that its period has to be integer multiples of the SAO period. The first factor determines that the period should be approximately 28 months, which is intermediate between 4-SAO and 5-SAO periods. It achieves an averaged period of 28 months by jumping between 4-SAO periods and 5-SAO periods. And it does so even if the solar forcing is held constant. These non-stationary jumps, of about 6 months from one period to another, account for most of the variability of the QBO period, and can probably account for the contradictory findings of correlation and anti-correlation with the SC depending on which segment of record one examines.

Nevertheless, there does exist SC influences on the mean QBO period. These effects are weak but are detectable in the model, and appear to be opposite to what was previously proposed. We offer an explanation below.

The partition of the whole QBO period into its easterly and its westerly parts in the lower stratosphere depends on the equatorial upwelling rate of the global Brewer-Dobson circulation. Fig. 9 shows the isentropic stream-function for the Brewer-Dobson circulation in the stratosphere in January. It shows a strengthened Brewer-Dobson circulation during SC-max conditions as compared to SC-min conditions. Under the SC-max conditions the planetary waves are more focused to mid and high latitudes, and there are more Stratospheric Sudden Warmings in the polar stratosphere during late winter (Labitzke, 1982; Camp and Tung, 2007). Consequently the polar stratosphere is warmer and the Brewer-Dobson circulation is more downward in mid to high latitudes (Cordero and Nathan, 2005). This could remotely force a stronger upwelling branch of the Brewer-Dobson circulation over the equator, which then slows the descent of the QBO shear zone and extends the QBO period. Because the QBO-induced secondary circulation itself is also upward for the easterly phase at the equator, the e-QBO is more vulnerable to slowing and eventual stalling, which usually occurs near 30 hPa (Plumb and Bell, 1982a, 1982b). Below the stalling level, the westerly phase persists without being replaced by the descending easterlies, leading to a longer westerly duration. In this model there is no local heating due to volcanic aerosols, and so the anomalous upwelling over the equator shown here is remotely forced by the breaking of planetary waves in the extra-tropics. This is the so-called "polar route" (Pascoe *et al.*, 2005).

This feature of the occasional stalling of the easterlies and the prolongation of the westerly duration below is absent in the 2D model of Mayr *et al*., (2003), which does not have planetary waves that interact with the mean flow altered by solar-cycle forcing. Consequently in their model the descent of the easterlies and westerlies are more uniform than here and than in the observed data. The prolongation of the w-QBO in the lower stratosphere is an important feature of the observed decadal variation of the QBO period because it delays the onset of the next westerly descent into the stratosphere by filtering out the westerly waves. In the absence of the westerly wave momentum deposition, the easterly duration is lengthened in the upper stratosphere. In the observational result of Fischer and Tung (2008), the decadal variation of the easterly duration at 15 hPa is tied to that of the westerly duration at 50 hPa. This feature is also seen in this model.

A second mechanism is the so-called “equatorial route” of local radiative heating by the increased solar flux in SC-max as compared to the SC-min. In this model the UV radiation of the SC forcing interacts with ozone most strongly in the stratopause region, and the resulting diabatic heating affects the propagation of the equatorial waves in the upper stratosphere and affects the wave forcing of the QBO. This solar perturbation serves to “kick” the QBO period from one SAO multiple into another, higher (on average) multiple. To test this hypothesis, we make another run by switching off the SC-ozone feedback. Ozone in the model is then not allowed to change as SC changes, but other interactions with dynamics are still allowed. When ozone concentration is fixed, the mean QBO period changes very little with solar flux, even for up to 15 times SC-max. This experiment suggests that the small positive dependence of QBO period on the strength of the solar flux we see in the model is mostly due to this “equatorial route”. Although much more work needs to be done to fully understand this mechanism, we do not believe it is worth the effort at this time given how small an effect it has on the QBO period under realistic levels of solar forcing.

Another mechanism for solar influence on the period of QBO was proposed by Cordero and Nathan (2005), who employed a model simulation to show that the QBO circulation is slightly stronger (weaker) during the SC-max (SC-min), resulting in a shorter (longer) QBO period arising from wave-ozone feedback. They argued that this leads to the required diabatic heating that slows down the descent rate of the equatorial QBO. This wave-ozone feedback is not included in our model.

In summary, we find two mechanisms of how a change in solar flux affects the period of the QBO. Both are weak under the current SC forcing—explaining perhaps about one to two months of the variability —but can nevertheless account for the tendency of positive correlation of the mean QBO period with the SC in models: (1) through a change in the strength of the Brewer-Dobson circulation by its effect on planetary waves, and (2) by local heating change in the upper stratosphere. The first mechanism is a remote mechanism, and is absent in 2D models without inter-annual change in planetary wave propagation and dissipation. The second mechanism is local, and affects the magnitude of the radiative heating perturbation that alters the wave forcing of the QBO. This effect is absent in models without ozone photochemistry. This mechanism responds to increasing solar forcing by changing the distribution of its period to less 4-SAO periods and more 5- SAO periods. The first mechanism, previously suggested, affects mainly the partition of the QBO into its easterly and westerly phases. Its effect on the QBO period is about one month or less. The second mechanism is effective only when the SC forcing is magnified 5 to 10 times.

7. Conclusions

It is well known that the polar stratosphere in winter is significantly more perturbed when the equatorial QBO is easterly than when it is westerly (Holton and Tan, 1980, 1982; Baldwin et al, 2001). A mechanism that can affect the period of the equatorial QBO, by altering the timing of the phase of the QBO relative to the polar winter, will therefore have a significant impact on the circulation of the entire stratosphere. The 11-year SC has often been cited as able to modulate the equatorial QBO period, especially its westerly duration in the lower stratosphere. Salby and Callaghan (2000), Soukharev and Hood (2001) and Pascoe *et al.*, (2005) found that the duration of the w-QBO in the lower stratosphere is lengthened during solar minima based on the observations. While confirming these results, Hamilton (2002) and Fischer and Tung (2008) found with longer datasets that perhaps the opposite may hold during other decades, which coincidentally did not have volcanic aerosol contamination. The record is not long enough for us to establish the behavior of the solar-cycle modulation of the QBO period in a clean stratosphere, although it is not clear if the volcanoes were the culprit. In the present model where there is no volcanic influence and long runs are possible, we find that the main variability of the QBO period is not related to the SC, but is an intrinsic property of the QBO itself. Quantum jumps of about six months between QBO periods occur in an apparently random fashion even when the variability in the solar forcing is suppressed in the model. In shorter segments of the record, such variability can give the appearance of instantaneous correlation or anti-correlation with the SC. Examples are shown in Fig. 10: both positive and negative instantaneous correlations with the SC can be found in short segments with durations comparable to those used in previous observational studies, while there is no statistically significant correlation of QBO period with the SC in the long records of 200 or even 400 model years of periodic forcing.

When the non-stationary variability of the QBO period is averaged out in a long enough run (200 years), there is a statistically significant positive correlation of the averaged QBO period with the solar forcing: the QBO period is lengthened during solar maxima, and that the increase in period is proportional to the solar-cycle forcing. This effect is weak and can be overwhelmed by the non-stationary behavior in shorter records. This finding may reconcile the contradictory findings of Salby and Callaghan (2000), Hamilton (2002) and Fischer and Tung (2008), using observation from FUB of various lengths that show either anti-correlation or no correlation of the QBO period with the SC.

Acknowledgements: This work was supported in part by NASA grants NAG1-1806 and NNG04GN02G to the California Institute of Technology. K. K. Tung's research was supported by

NSF grants ATM 0332364 and ATM 0808375 to University of Washington. We would like to thank A. Ruzmaikin and J. Feynman for useful discussions. We also acknowledge help in improving the paper from M. C. Liang, N. Heavens, X. Guo, A. Soto, T. Lee, X. Zhang, P. S. Jiang, Y. C. Chen, D. Yang, and C. D. Camp.

References

Baldwin, M. P., L. J. Gray, T. J. Dunkerton, K. Hamilton, P. H. Haynes, W. J. Randel, J. R. Holton, M. J. Alexander, I. Hirota, T. Horinouchi, D. B. A. Jones, J. S. Kinnersley, C. Marquardt, K. Sato, and M. Takahashi, 2001: The quasi-biennial oscillation, *Rev. Geophys.*, *39*(2), 179-229.

Camp, C. D., and K. K. Tung, 2007: The influence of the solar cycle and QBO on the late-winter stratospheric polar vortex, *J. Atmos. Sci.*, *64*(4), 1267-1283.

Cordero, E. C., and T. R. Nathan, 2005: A new pathway for communicating the 11-year solar cycle signal to the QBO, *Geophys. Res. Lett.*, *32*(18), art. no L18805.

Dunkerton, T. J., 1983: Modification of stratospheric circulation by race constituent changes?, *J. Geophys. Res.*, *88*, 10,831-10,836.

Dunkerton, T. J., 1997: The role of gravity waves in the quasi-biennial oscillation, *J. Geophys. Res.*, *102*(D22), 26053-26076.

Fischer, P., and K. K. Tung, 2008: A reexamination of the QBO period modulation by the solar cycle, *J. Geophys. Res.-Atmos.*, *113*(D07114), doi:10.1029/2007JD008983.

Hamilton, K., 2002: On the quasi-decadal modulation of the stratospheric QBO period, *J. Climate*, *15*(17), 2562-2565.

Hasebe, F., 1983: Interannual variations of global total ozone revealed from Nimbus 4-Buv and Ground-based observations, *J. Geophys. Res.*, *88*(NC11), 6819-6834.

Holton, J. R., and R. S. Lindzen, 1972: Updated theory for Quasi-Biennial Cycle of tropical stratosphere, *J. Atmos. Sci.*, *29*(6), 1076-1080.

Holton, J. R., and H. C. Tan, 1980: The influence of the equatorial quasi-biennial oscillation on the global circulation at 50 mb, *J. Atmos. Sci., 37*(10), 2200-2208.

Holton, J. R., and H. C. Tan, 1982: The quasi-biennial oscillation in the northern hemisphere lower stratosphere, *J. Meteor. Soc. Japan, 60*(1), 140-148.

Jackman, C., E. L. Fleming, S. Chandra, D. B. Considine, and J. E. Rosenfield, 1996: Past, present, and future modeled ozone trends with comparisons to observed trends, *J. Geophys. Rev., 101(D22)*, 28753-28767.

Kalnay, E., M. Kanamitsu, R. Kistler, W. Collins, D. Deaven, L. Gandin, M. Iredell, S. Saha, G. White, J. Woollen, Y. Zhu, M. Chelliah, W. Ebisuzaki, W. Higgins, J. Janowiak, K. C. Mo, C. Ropelewski, J. Wang, A. Leetmaa, R. Reynolds, R. Jenne, and D. Joseph, 1996: The NCEP/NCAR 40-year reanalysis project, *Bull. Am. Meteorol. Soc.*, *77*(3), 437-471.

Kinnersley, J. S., and R. S. Harwood, 1993: An isentropic 2-dimensional model with an interactive parameterization of dynamical and chemical planetary-wave fluxes, *Q. J. R. Meteorol. Soc.*, *119*(513), 1167-1193.

Kinnersley, J. S., and S. Pawson, 1996: The descent rates of the shear zones of the equatorial QBO, *J. Atmos. Sci*., *53*(14), 1937-1949.

Kistler, R., E. Kalnay, W. Collins, S. Saha, G. White, J. Woollen, M. Chelliah, W. Ebisuzaki, M. Kanamitsu, V. Kousky, H. van den Dool, R. Jenne, and M. Fiorino, 2001: The NCEP-NCAR 50-year reanalysis: Monthly means CD-ROM and documentation, *Bull. Am. Meteorol. Soc.*, 247-267.

Kuai, L., R. L. Shia, X. Jiang, K. K. Tung, and Y. L. Yung, 2008: Non-stationary Synchronization of Equatorial QBO with SAO in Observation and in Model, Submitted to *J. Atmos. Sci.* (submitted).

Mayr, H. G., J. G. Mengel, D. P. Drob, H. S. Porter, and K. L. Chan, 2003: Modeling studies with QBO: I. Quasi-decadal oscillation, *J. Atmos. Terr. Phys.*, *65*(8), 887-899.

Mayr, H. G., J. G. Mengel, D. P. Drob, H. S. Porter, and K. L. Chan, 2003: Modeling studies with QBO: II. Quasi-decadal oscillation, *J. Atmos. Terr. Phys.*, *65*(8), 901-916.

Oltmans, S.J., and J. London, 1982: The Quasi-Biennial Oscillation in Atmospheric Ozone, *J. Geophys. Res.*, *87*(NC11), 8981-8989.

Pascoe, C. L., L. J. Gray, S. A. Crooks, M. N. Juckes, and M. P. Baldwin, 2005: The quasi-biennial oscillation: Analysis using ERA-40 data, *J. Geophys. Res.*, *110*(D8), D08105, doi:10.1029/ 2004JD004941.

Pawson, S., and M. Fiorino, 1998: A comparison of reanalyses in the tropical stratosphere. Part 2: The quasi-biennial oscillation, *Clim. Dyn.*, *14*(9), 645-658.

Plumb, R. A., and R. C. Bell, 1982a: Equatorial waves in steady zonal shear flow, *Q. J. R. Meteorol. Soc.*, *108*(456), 313-334.

Plumb, R. A., and R. C. Bell, 1982b: A model of the quasi-biennial oscillation on an equatorial beta-plane, *Q. J. R. Meteorol. Soc.*, *108*(456), 335-352.

Randel, W.J., and F. Wu, 1996: Isolation of the ozone QBO in SAGE II data by singular-value decomposition, *J. Atmos. Sci.*, *53*(17), 2546-2559.

Salby, M. L., and P. F. Callaghan, 2000: Connection between the solar cycle and the QBO: The missing link, *J. Climate*, *13*(14), 2652-2662.

Soukharev, B. E., and L. L. Hood, 2001: Possible solar modulation of the equatorial quasi-biennial oscillation: Additional statistical evidence, *J. Geophys. Res.*, *106*(D14), 14,855-14,868.

Uppala S. M. , Kallberg P. W. , Simmons A. J. , Andrae U. , Da Costa Bechtold V. , Fiorino M. , Gibson J. K. , Haseler J. , Hernandez A. , Kelly G. A. , Li X. , Onogi K. , Saarinen S. , Sokka N. , Allan R. P. , Andersson E. , Arpe K. , Balmaseda M. A. , Beljaars A. C. M. , Van De Berg L. , Bidlot J. , Bormann N. , Caires S. , Chevallier F. , Dethof A. , Dragosavac M. , Fisher M. , Fuentes M. , Hagemann S. , Holm E. , Hoskins B. J. , Isaksen L. , Janssen P. A. E. M. , Jenne R. , Mcnally A. P. , Mahfouf J.-F. , Morcrette J.-J. , Rayner N. A., Saunders R. W. , Simon P. , Sterl A. , Trenberth K. E. , Untch A. , Vasiljevic D. , Viterbo P., and Woollen J., 2005: The ERA-40 re-analysis, *Quart. J. Roy. Meteor. Soc.*, *131*, 2961-3012.

Zawodny, J.M., and M.P. McCormick, 1991: Stratospheric Aerosol and Gas Experiment-Ii Measurements of the Quasi-Biennial Oscillations in Ozone and Nitrogen-Dioxide, *J. Geophy. Res.*, *96*(D5), 9371-9377.

Figure Captions

Figure 1. Height-time cross-section of the monthly mean ERA-40 zonal wind (top two panels). In the lower two panels, the zonal wind in the upper three levels (1-3 hPa) are replaced by its seasonal climatology, which removes the QBO and shows the SAO more clearly.

Figure 2. QBO period in ERA-40 data at 5 hPa. (a) QBO period counted in units of SAO period (left scale). The solid curve at the bottom is the solar cycle index (W m^{-2}) (right scale). (b) The histogram of the QBO period, counting the number of occurrences when the QBO period is 4-SAO period and when it is 5-SAO period. (c) The average QBO period as a function of pressure level. (*) denotes the QBO that started in 1962, (+) that started in 1997 and the diamonds for the mean of all QBOs in the ERA-40 record.

Figure 3. Height-time cross-section of zonal mean zonal wind for1×SC-vary case from year 126 to year 172.

Figure 4. Same as Fig. 2 but from model results for the 1×SC-vary case. The solid curve is the solar index as Fig. 2 but repeating the data from 1964 to 1995 to cover 400 years. Here we choose 46 year out of 400 year run, from year 126 to year 172, for the purpose of comparing with the ERA-40 period. In (c) (*) represents the QBO during year 162 and (+) represents the QBO during year 128. Diamond represents the mean QBO periods during the 46 years.

Figure 5. The histogram of the QBO period, counting the number of occurrences when the QBO period is 4-SAO period and when it is 5-SAO period: (a) over the 400 years period; (b)-(d) different smaller time segments of 20 QBO periods, about 40-46 years.

Figure 6. Time-height section of the equatorial monthly-mean zonal wind component (in m/s) from the THINAIR model simulation. The individual QBO period is synchronized with SAO near the stratopause. The black line is the zero-wind line. (a) 15×SC-min perpetual condition; (b) 10×SC-min perpetual condition; (c) SC-mean perpetual condition; (d) 10×SC-max perpetual condition; (e) 15×SC-max perpetual condition.

Figure 7. The histogram of the QBO period—the number of occurrences when a QBO period is 4-SAO or 5-SAO periods—in model runs for various perpetual solar cycle forcing. (a) 15×SC-min; the resulting averaged QBO period is 24.64 months; (b) 10×SC-min; the averaged QBO period is 25.66 months; (c) SC-mean; the averaged QBO period is 27.20 months; (d) 5×SC-max; the averaged QBO period is 26.67 months; (e) 10×SC-max; the averaged QBO period is 28.43 months; (f) 15×SC-max; the averaged QBO period is 29.04 months.

Figure 8. QBO period averaged over the model run, as a function of the solar forcing, in units of SC-max. (a) The QBO period at various pressure levels from 10 hPa to 80 hPa; lines mostly overlap, showing not much vertical variation. Easterly duration is shown with (*) and westerly duration with (+) at (b) 10 hPa, (c) 20 hPa, (d) 30 hPa, (e) 50 hPa, (f) 80 hPa.

Figure 9. (a) Mass stream function on isentropic surfaces in units of 10^9 kg s^{-1} under SC-min condition. (b) The difference between the composites of the 10×SC-max and 10×SC-min. Both figures are for Jan.

Figure 10. QBO period as a function of years in the 400-year periodic solar cycle run. The TSI index is shown in solid line with the right-hand scale. The various panels are segments of the run of 40-46 years each (about 20 QBOs). The correlation of the QBO period with the TSI index is marked for each period.

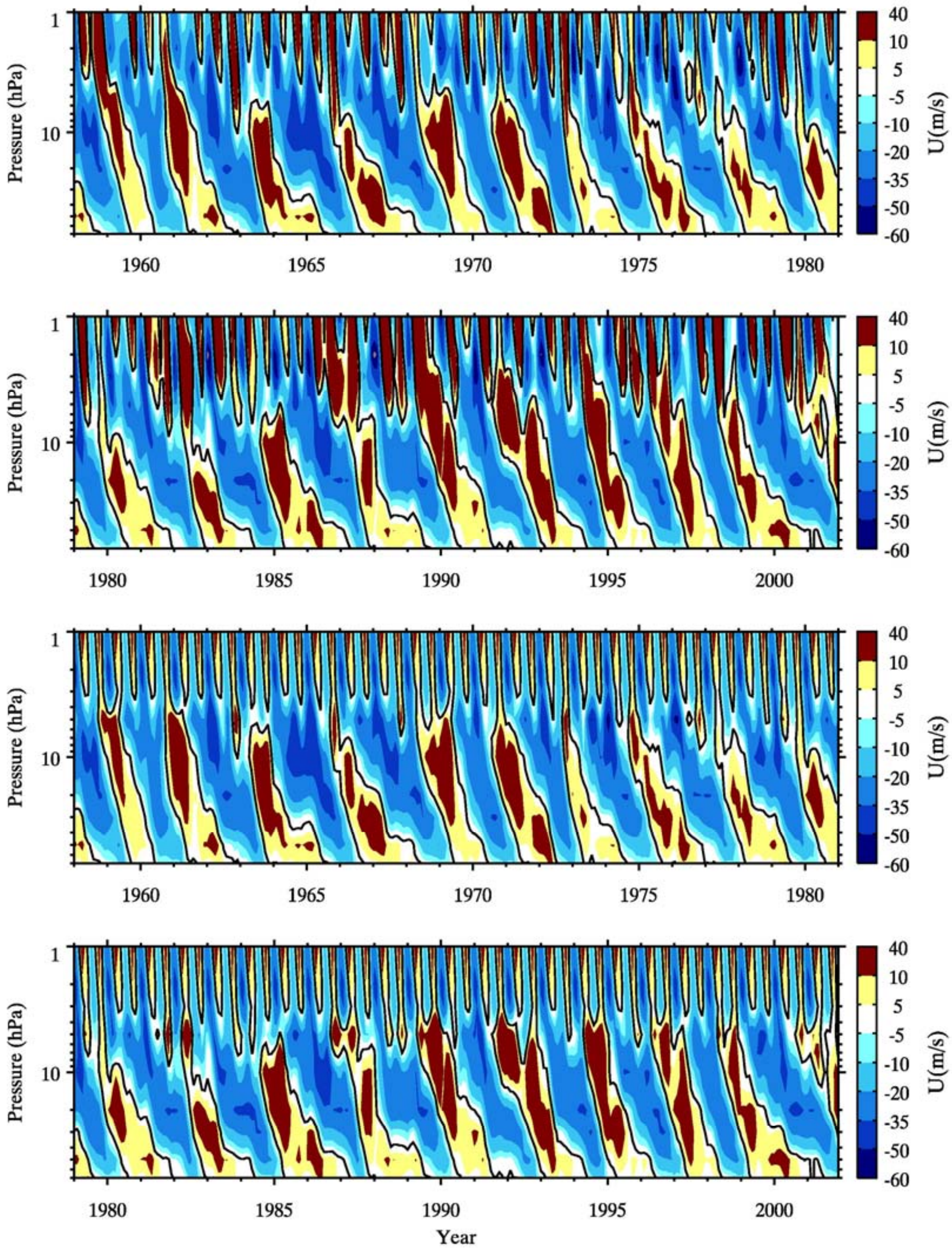

Figure 1. Height-time cross-section of the monthly mean ERA-40 zonal wind (top two panels). In the lower two panels, the zonal wind in the upper three levels (1-3 hPa) are replaced by its seasonal climatology, which removes the QBO and shows the SAO more clearly.

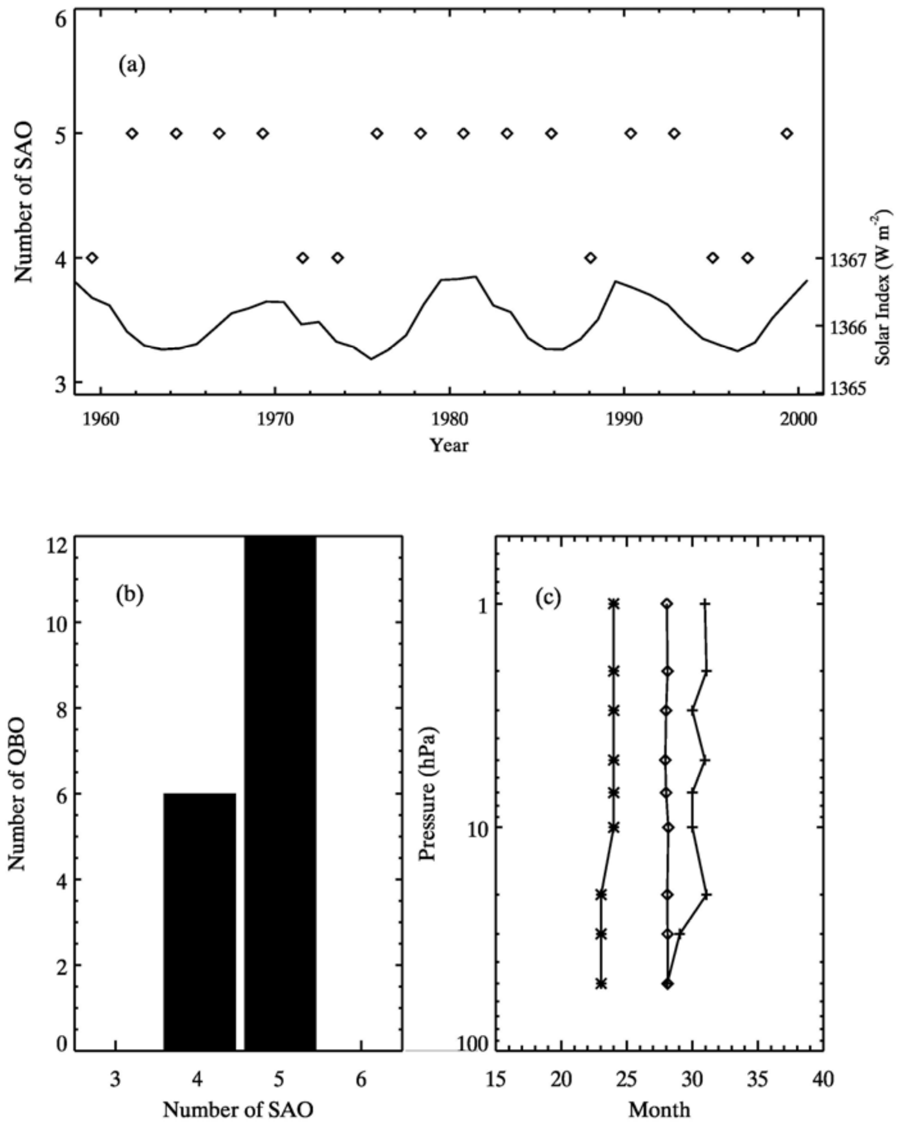

Figure 2. QBO period in ERA-40 data at 5 hPa. (a) QBO period counted in units of SAO period (left scale). The solid curve at the bottom is the solar cycle index (W m^{-2}) (right scale). (b) The histogram of the QBO period, counting the number of occurrences when the QBO period is 4-SAO period and when it is 5-SAO period. (c) The average QBO period as a function of pressure level. (*) denotes

the QBO that started in 1962, (+) that started in 1997 and the diamonds for the mean of all QBOs in the ERA-40 record.

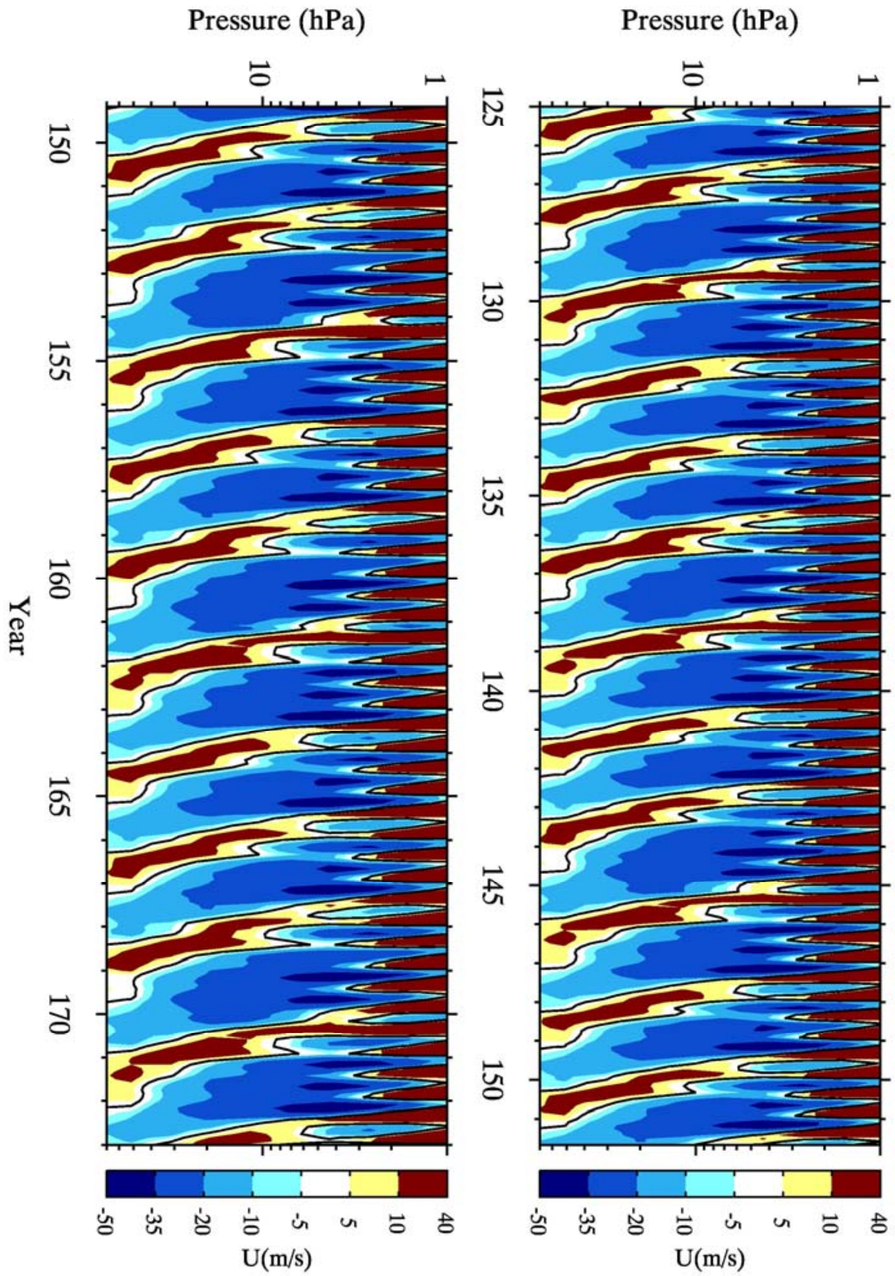

Figure 3. Height-time cross-section of zonal mean zonal wind for1×SC-vary case from year 126 to year 172.

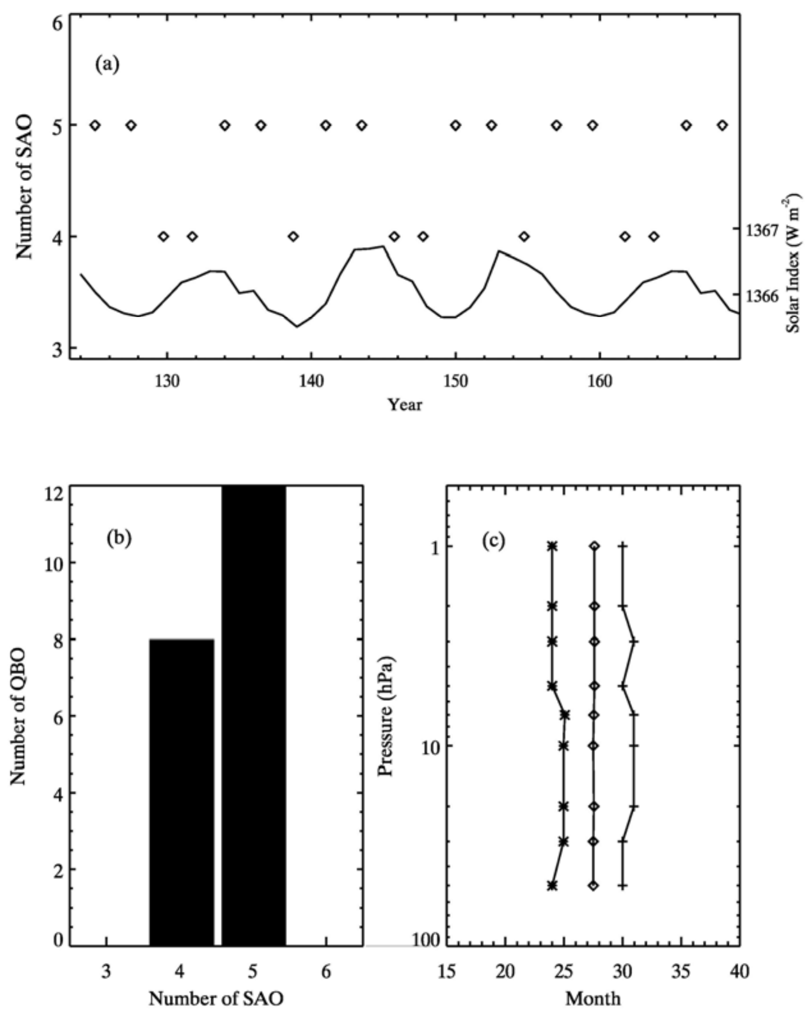

Figure 4. Same as Fig. 2 but from model results for the 1×SC-vary case. The solid curve is the solar index as Fig. 2 but repeating the data from 1964 to 1995 to cover 400 years. Here we choose 46 year out of 400 year run, from year 126 to year 172, for the purpose of comparing with the ERA-40 period. In (c) (*) represents the QBO during year 162 and (+) represents the QBO during year 128. Diamond represents the mean QBO periods during the 46 years.

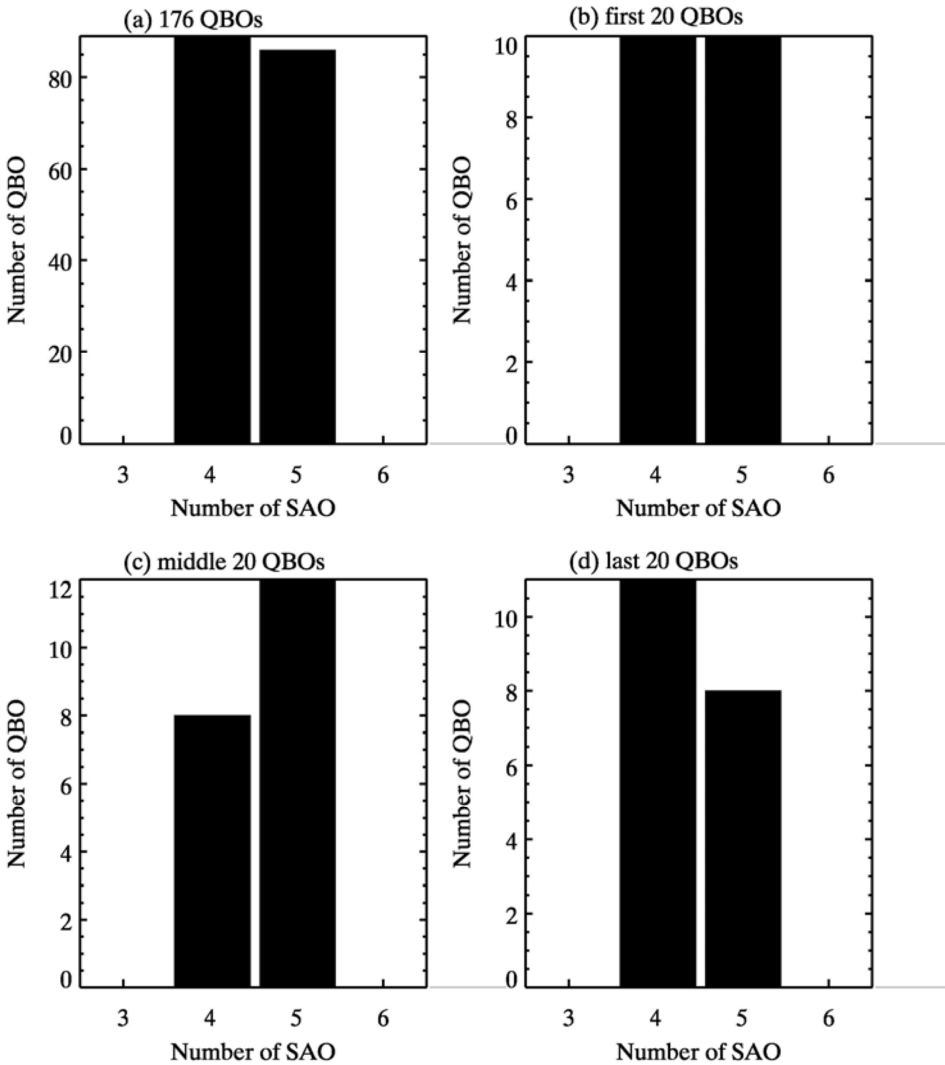

Figure 5. The histogram of the QBO period, counting the number of occurrences when the QBO period is 4-SAO period and when it is 5-SAO period: (a) over the 400 years period; (b)-(d) different smaller time segments of 20 QBO periods, about 40-46 years.

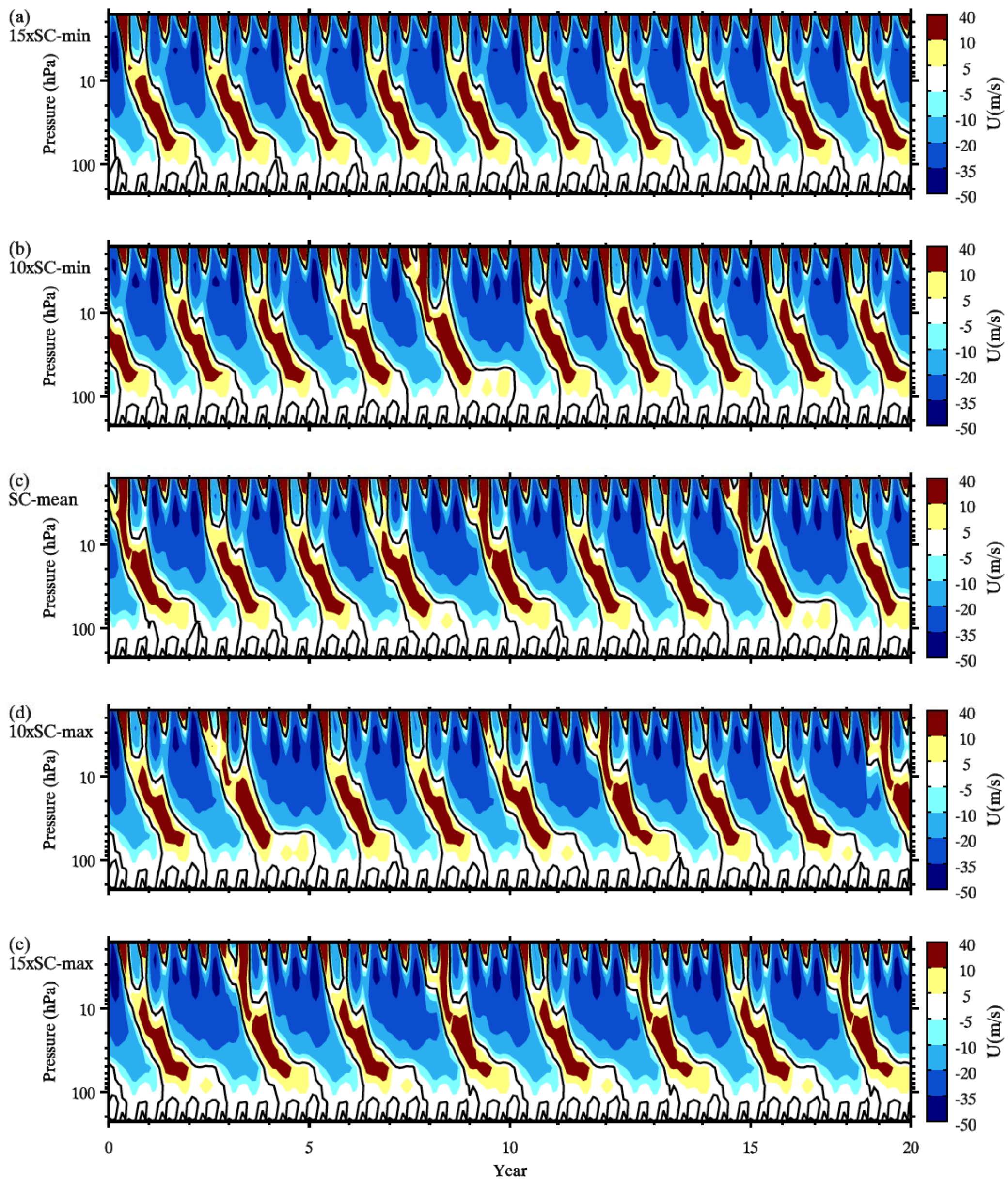

Figure 6. Time-height section of the equatorial monthly-mean zonal wind component (in m/s) from the THINAIR model simulation. The individual QBO period is synchronized with SAO near the stratopause. The black line is the zero-wind line. (a) 15×SC-min perpetual condition; (b) 10×SC-min perpetual condition; (c) SC-mean perpetual condition; (d) 10×SC-max perpetual condition; (e) 15×SC-max perpetual condition.

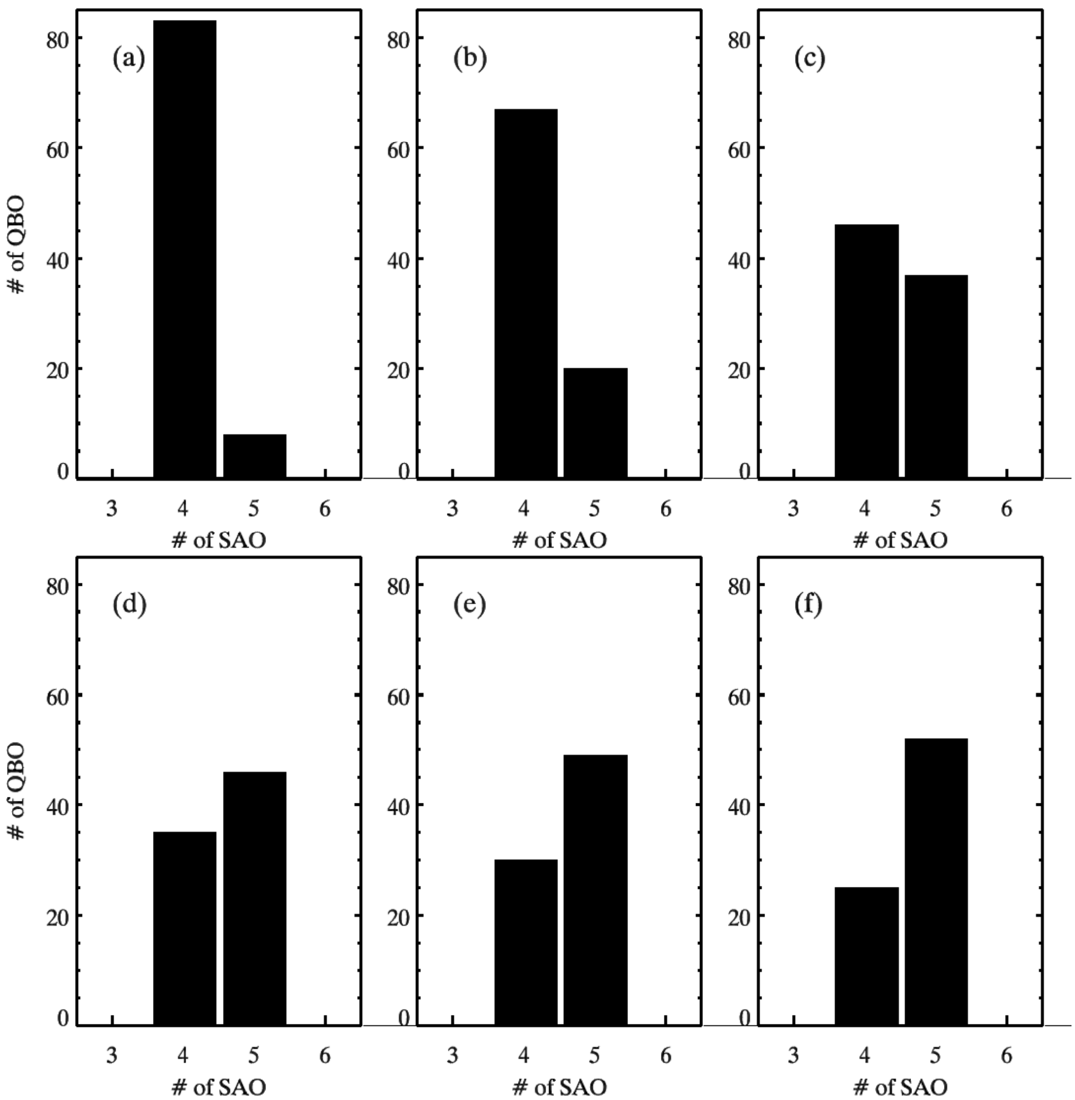

Figure 7. The histogram of the QBO period—the number of occurrences when a QBO period is 4-SAO or 5-SAO periods—in model runs for various perpetual solar cycle forcing. (a) 15×SC-min; the resulting averaged QBO period is 24.64 months; (b) 10×SC-min; the averaged QBO period is 25.66 months; (c) SC-mean; the averaged QBO period is 27.20 months; (d) 5×SC-max; the averaged QBO period is 26.67 months; (e) 10×SC-max; the averaged QBO period is 28.43 months; (f) 15×SC-max; the averaged QBO period is 29.04 months.

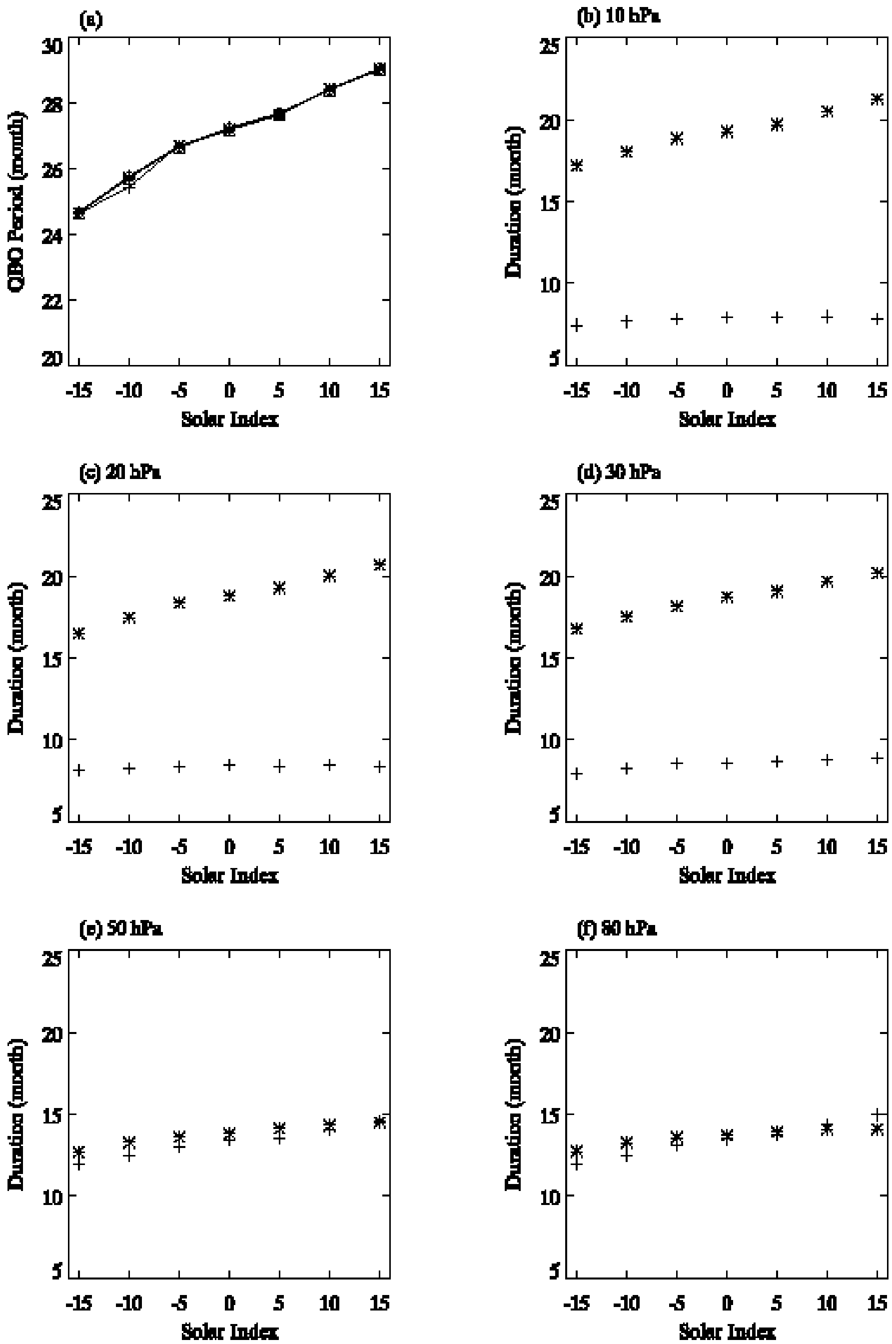

Figure 8. QBO period averaged over the model run, as a function of the solar forcing, in units of SC-max. (a) The QBO period at various pressure levels from 10 hPa to 80 hPa; lines mostly overlap, showing not much vertical variation. Easterly duration is shown with (*) and westerly duration with (+) at (b) 10 hPa, (c) 20 hPa, (d) 30 hPa, (e) 50 hPa, (f) 80 hPa.

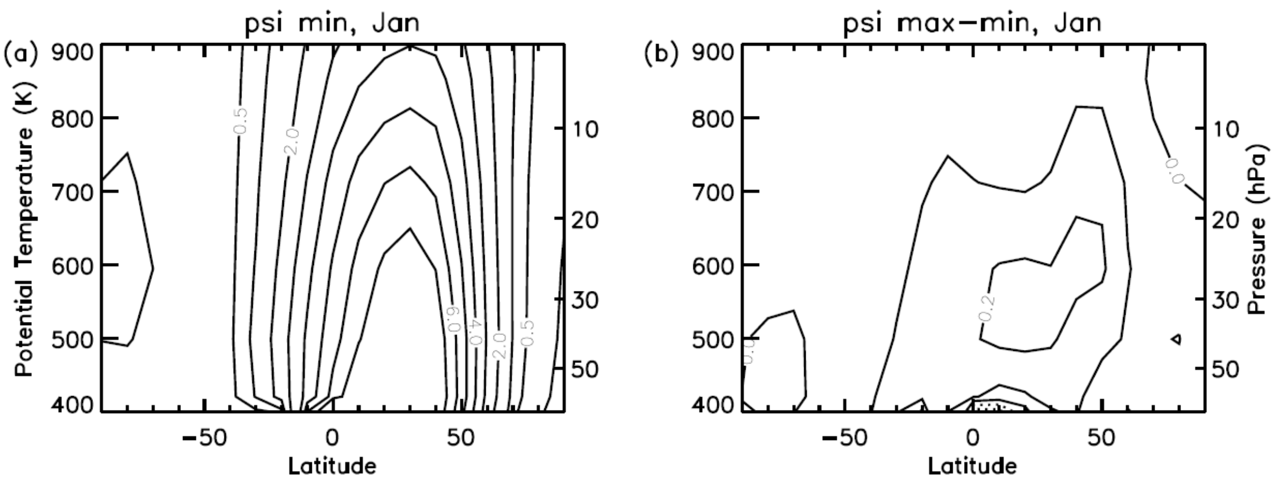

Figure 9. (a) Mass stream function on isentropic surfaces in units of 10^9 kg s^{-1} under SC-min condition. (b) The difference between the composites of the 10×SC-max and 10×SC-min. Both figures are for Jan.

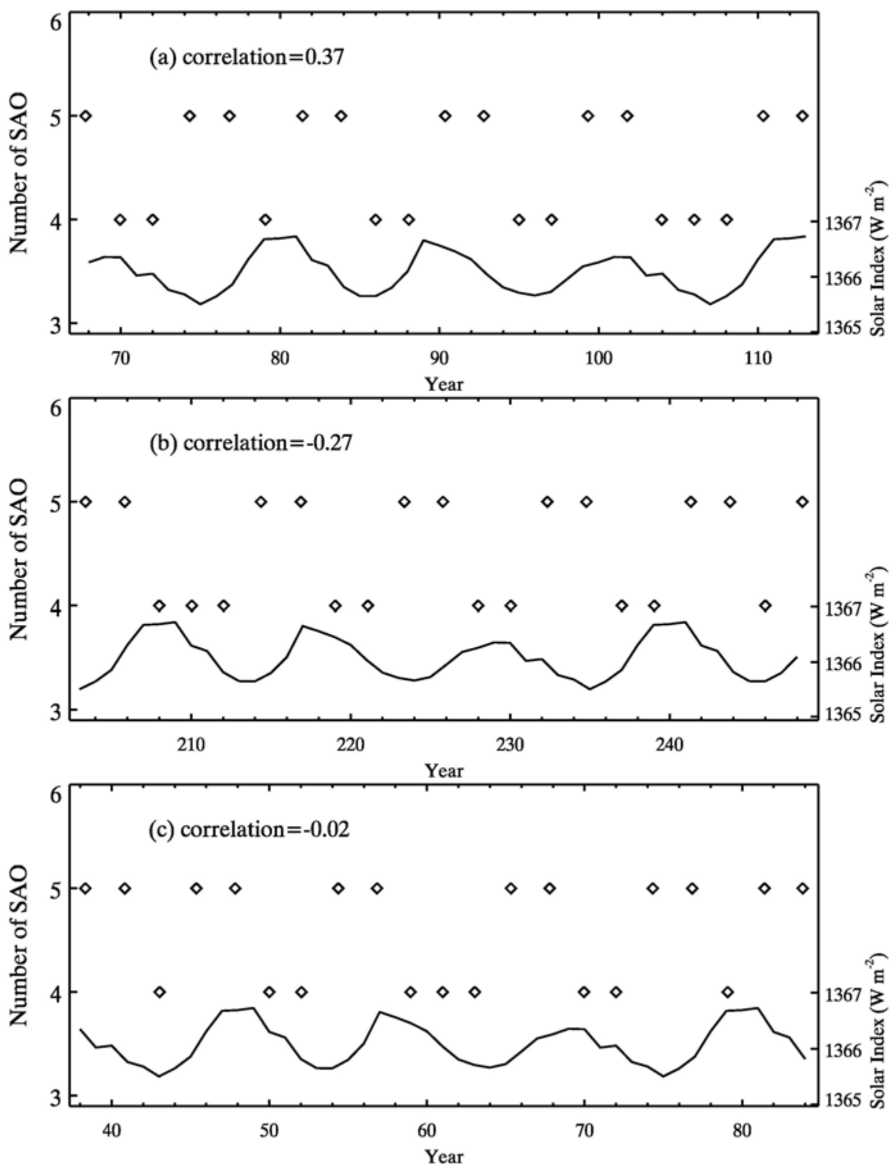

Figure 10. QBO period as a function of years in the 400-year periodic solar cycle run. The TSI index is shown in solid line with the right-hand scale. The various panels are segments of the run of 40-46 years each (about 20 QBOs). The correlation of the QBO period with the TSI index is marked for each period.